Hippocampal and cortical atrophy predict dementia in subcortical ischemic vascular disease

G. Fein, PhD, **V. Di Sclafani, MPH**, **J. Tanabe, MD**, **V. Cardenas, PhD**, **M.W. Weiner, MD**, **W.J. Jagust, MD**, **B.R. Reed, PhD**, **D. Norman, MD**, **N. Schuff, PhD**, **L. Kusdra**, **T. Greenfield**, and **H. Chui, MD**

Neurobehavioral Research, Inc. (Dr. Fein and V. Di Sclafani); Psychiatry Research (Dr. Cardenas) and Magnetic Resonance Unit (Drs. Tanabe, Weiner, and Schuff, and L. Kusdra and T. Greenfield), Department of Veterans Affairs Medical Center; the Departments of Radiology (Drs. Tanabe, Cardenas, Weiner, Norman, and Schuff) and Psychiatry (Dr. Weiner), University of California, San Francisco; the Center for Functional Imaging (Dr. Jagust), Lawrence Berkeley Laboratory, the Department of Neurology (Drs. Jagust and Reed), University of California, Davis; and the Department of Neurology (Dr. Chui), University of Southern California, Los Angeles.

Abstract

Background—The cause of dementia in subcortical ischemic vascular disease (SIVD) is controversial.

Objectives—To determine whether cognitive impairment in SIVD 1) correlates with measures of ischemic brain injury or brain atrophy, and/or 2) is due to concomitant AD.

Methods—Volumetric MRI of the brain was performed in 1) elderly subjects with lacunes (L) and a spectrum of cognitive impairment—normal cognition (NC+L, n = 32), mild cognitive impairment (CI+L, n = 26), and dementia (D+L, n = 29); 2) a comparison group with probable AD (n = 28); and 3) a control group with normal cognition and no lacunes (NC). The authors examined the relationship between the severity of cognitive impairment and 1) volume, number, and location of lacunes; 2) volume of white matter signal hyperintensities (WMSH); and 3) measures of brain atrophy (i.e., hippocampal, cortical gray matter, and CSF volumes).

Results—Among the three lacune groups, severity of cognitive impairment correlated with atrophy of the hippocampus and cortical gray matter, but not with any lacune measure. Although hippocampal atrophy was the best predictor of severity of cognitive impairment, there was evidence for a second, partially independent, atrophic process associated with ventricular dilation, cortical gray matter atrophy, and increase in WMSH. Eight autopsied SIVD cases showed variable severity of ischemic and neurofibrillary degeneration in the hippocampus, but no significant AD pathology in neocortex. The probable AD group gave evidence of only one atrophic process, reflected in the severity of hippocampal atrophy. Comparison of regional neocortical gray matter volumes showed sparing of the primary motor and visual cortices in the probable AD group, but relatively uniform atrophy in the D+L group.

Conclusions—Dementia in SIVD, as in AD, correlates best with hippocampal and cortical atrophy, rather than any measure of lacunes. In SIVD, unlike AD, there is evidence for partial independence between these two atrophic processes. Hippocampal atrophy may result from a mixture of ischemic

Address correspondence and reprint requests to Dr. Helena Chui, Geriatric Neurobehavior and Alzheimer Center, 800 Annex West, 7601 East Imperial Highway, Downey, CA 90242; e-mail: chui@hsc.usc.edu.

and degenerative pathologies. The cause of diffuse cortical atrophy is not known, but may be partially indexed by the severity of WMSH.

Subcortical ischemic vascular disease (SIVD) is characterized by lacunar infarcts and deep white matter changes. The proportion of vascular dementia (VaD) attributed to SIVD ranges from 36 to 50%, with higher rates noted among African Americans[1] and Asian Americans[2] than whites.[3,4] A few studies report risk of dementia to be higher among subjects with lacunar infarcts versus other subtypes of stroke,[4] and among patients with AD with concomitant lacunar versus large-artery infarcts.[5] Thus, SIVD is an important subtype of VaD either alone or in combination with AD.

Despite its prevalence, the pathways leading to dementia in SIVD remain controversial. Several mechanisms have been proposed. According to the lacunar hypothesis, cognitive impairment results from increasing number and volume of lacunes, especially when located strategically within frontal subcortical loops.[6,7] In Binswanger syndrome, a subtype of SIVD, widespread stenosis of small arteries is postulated to result in chronic ischemia of the periventricular and deep white matter.[8] Some investigators suggest that dementia in SIVD is due to coexisting AD. [9]

Attempts have been made to correlate quantitative measures of ischemic lesions and brain atrophy with dementia. Atrophy of the hippocampus and medial temporal lobe, anatomic regions highly susceptible to neurofibrillary degeneration, are characteristically observed in AD.[10-12] Previous investigators have correlated dementia in SIVD with the severity of ventricular enlargement,[3,13-15] white matter lesions,[14,16-18] cerebral hypoperfusion,[13,18,19] and number, but not necessarily volume, of lacunes.[3,16,19] One group has noted the presence of hippocampal atrophy in VaD, as well as AD.[20] With the exception of the studies of hippocampal atrophy, severity of ischemic lesions and brain atrophy were assessed using semiquantitative measures. Atrophy specifically affecting neocortical gray matter has not been previously examined.

In the current study, we examined the relation between cognitive impairment and volumetric measures of brain tissue compartments, including lacunes. Two major questions were examined. First, among individuals with lacunes, what neuroimaging measures differentiate individuals who are cognitively normal from those who are mildly impaired and from those who are demented? Second, is dementia among patients with lacunes simply due to concomitant AD?

Methods

Subjects

Subjects comprise a convenience sample recruited from a university dementia clinic and a Department of Veterans Affairs system of hospital and clinics. Normal controls were recruited from the community. Individuals with 1) a history of small stroke, 2) a radiologic report of a small infarct, 3) a diagnosis of probable AD, or 4) no history of significant cognitive impairment were invited to participate in the study. The research protocol was approved by the Institutional Review Boards at UC San Francisco and UC Davis. All subjects or their legal guardians gave written informed consent before participating in the study.

Evaluation of all subjects included complete medical history, activities of daily living, physical examination, neurologic examination, serum chemistry, blood count, vitamin B_{12}, syphilis serology, and thyroid function tests. Level of cognitive function was assessed using the Folstein Mini-Mental State Examination (MMSE)[21] and the Clinical Dementia Rating scale (CDR).

[22] A head MRI was obtained using a standardized protocol at a single centralized site (Magnetic Resonance Unit, Department of Veterans Affairs medical Center, UCSF).

Exclusion criteria included age younger than 55 years, non-English speaking, severe dementia (CDR > 2), evidence of alcohol or substance abuse, head trauma with loss of consciousness lasting longer than 15 minutes, severe medical illness, neurologic or psychiatric disorders, or currently taking medications likely to affect cognitive function. In addition, subjects were excluded if the MRI showed evidence of cortical infarction, hemorrhage, or structural brain disease other than atrophy, lacunes, or white matter signal hyperintensities (WMSH).

Subjects with lacunes had at least one lacune identified on MRI by a neuroradiologist (D.N.) in the subcortical gray or white matter. Subjects with probable AD (prAD) did not have any lacunes and met National Institute of Neurological and Communicative Disorders and Stroke–AD and Related Disorders Association criteria for prAD.[23] None of the healthy controls had lacunes. Subjects with lacunes (L) were divided into three groups based on the CDR: 1) cognitively normal (CN+L, CDR = 0, n = 32), 2) cognitively impaired (CI+L, CDR = 0.5, n = 26), or demented (D+L, CDR = 1 or 2, n = 29).

The D+L group was compared to a group of subjects with prAD (n = 28), with comparable distributions of age, gender, and MMSE scores. The CN+L, CI+L, and D+L were each compared to a subset of cognitively normal controls (NC), chosen to have a comparable age and gender distribution. Some subjects served as normal controls for more than one lacune group (6 controls were used in two comparisons, 11 were used in three comparisons, and 10 were used in four comparisons).

MRI acquisition

The entire brain was imaged with a 1.5 Tesla MR system (Siemens Vision, Erlangen, Germany) using a head coil with quadrature detection. The brain imaging protocol involved 1) a sequence yielding proton density (PD) and T2-weighted spin-echo axial images (repetition time [TR]/echo time [TE]1/TE2 2500/20/80 msec; 1 number of excitations [NEX]), 3 mm slice thickness with no slice gap, in-plane resolution 0.94×0.94 mm^2, and 2) a sequence yielding T1-weighted coronal images (TR/TE 10/4 msec; 1 NEX), 1×1 mm^2 in-plane resolution, with contiguous 1.4 mm thick slices.

Image analysis

Tissue volumes were determined by a technician using computer-assisted methods, but blind to clinical information, including diagnosis. The T1, PD, and T2-weighted spin-echo images were used for segmentation into tissue categories. The segmentation process consisted of stripping the skull from the images, coregistering the T1-weighted images to the spin-echo data set,[24] and inhomogeneity filtering of the spin-echo images. Very conservative samples of CSF, white matter, and gray matter were chosen as seeds for a K-Means cluster analysis[25] in order to segment the entire brain into these tissue compartments. This initial automated process was followed by manual editing of the axial segmented images on a slice by slice basis. A trained technician separated cortical from subcortical gray matter, and ventricular from sulcal CSF. The technician also reclassified pixels as WMSH that had been classified by the K-means procedure as either gray matter or CSF due to their relative hyperintensity, but were clearly white matter by anatomic location.

Lesions on MRI were classified as lacunes based on signal characteristics, location, and size, using a definition similar to the Cardiovascular Health Study.[26] The operator viewed the coregistered PD, T2, and T1-weighted 3 mm thick axial gray scale images from the most inferior slice on which the thalamus was visible through the most superior slice of the brain.

The boundaries of the lacune were hand-drawn using the PD and T2-weighted image. The location of the lacune was recorded within white matter, caudate, putamen, globus pallidus, or thalamus. The final lacune markings were reviewed by a neuroradiologist (D.N.).

With the few exceptions noted below, lacunes were defined as lesions 3 to 15 mm in length, hyperintense relative to CSF on the PD image, and located in the subcortical gray and white matter. There were two exceptions. Large cystic lesions (bright on T2-weighted, but isointense relative to CSF on PD images) were classified as cystic lacunes unless they were located near the anterior commissure or below the putamen, in which case they were classified as perivascular spaces.[27] Within the white matter, only cystic lacunes were volumed. Noncystic lacunes in white matter were included as WMSH.

Figure 1 presents the MR and segmented images of an 86-year-old male D+L subject, illustrating the delineation of lacunes and WMSH, as well as cortical gray matter, white matter, and sulcal and ventricular CSF. The number of pixels in each tissue category was converted to a percentage of the intracranial vault (ICV = the total of all tissue categories). All statistical analyses were performed on data expressed as percent ICV data (i.e., controlling for subject differences in ICV). The hippocampal data and lacune volume data, however, are presented as volumes in mm^3 in tables 1 and 2 and figure 4, to facilitate comparison with other studies.

Hippocampal voluming

Hippocampal voluming was originally planned as a substudy, separate from analysis of the segmented images. Hippocampal voluming was performed on 65 subjects with lacunes (24 CN +L, 18 CI+L, 23 D+L), on control samples with comparable age and gender distributions as each lacune group, and on 18 prAD subjects with comparable age, gender, and MMSE distributions as the D+L group (see table 1). Hippocampal volumes were measured on T1-weighted images, reformatted to be perpendicular to the long axis of each subject's hippocampus (left and right reformatted separately). The hippocampal areas on each reformatted MRI slice were then drawn using the methods and anatomic boundaries described by Watson et al.,[28] as in our previous publication.[29] The hippocampal voluming was performed on 1.4 mm slices from the first visible anterior portion of the hippocampal head (the pes hippocampus) through the most posterior aspect of the hippocampus (the hippocampal tail) at the point of the separation of the crus of the fornix from the fimbria of the hippocampus (excluded at this level are the crus of the fornix, the isthmus of the cingulate gyrus, and the parahippocampal gyrus). We have previously established an interoperator reliability of 0.81 for this hippocampal voluming method.[29]

Regional analysis using the Talairach coordinate system

In the Talairach coordinate system, the brain is subdivided into 864 compartments: 12 in the superior–inferior plane (8 superior to the anterior–posterior commissure [AC–PC] line, and 4 inferior to the AC-PC line), 9 in the anterior–posterior direction (4 anterior to the AC point, 4 posterior to the PC point, and 1 between the AC and the PC), and 4 compartments in each direction lateral to the interhemispheric fissure (8 compartments total). The Brodmann areas encompassed by each of these 864 voxels are identified in the 1988 Talairach atlas.[30]

From within the frontal, parietal, occipital, temporal, and limbic areas of the brain, we defined 16 cortical regions of interest (ROI) by their corresponding Brodmann areas. These regions (and the Brodmann areas they encompass) were the orbital frontal and frontal pole (10, 11), lateral frontal (45, 46, 47), posterior frontal (6, 8, 44), superior frontal (8, 9), primary motor (4), primary sensory (1, 2, 3), lateral parietal (39, 40), mesial parietal (5, 7, 23, 31), anterior occipital (37), visual association (17, 18, 19), anterior temporal (21, 38), superior temporal (34, 41, 42), inferior temporal (20), and the limbic lobe (24, 29). The method of transformation of

each subject's T1-weighted image to the Talairach coordinate system involved several steps. First, the skull and meninges were removed, and the midpoints of the AC and the PC and the pontomedullary sulcus were marked. The brain was then rotated (using a modification of Bedell's method)[31] to an orientation where the AC and PC points lie on the same axial plane, and the interhemispheric fissure (IF) lies on a single sagittal plane.

The transformation to the Talairach coordinate system involved piecewise linear transformations of 12 compartments for each subject's brain. The 12 compartments were bounded by the IF, the plane perpendicular to the IF (yet containing the AC and PC points), the plane through the AC point perpendicular to the AC-PC plane and the IF, the plane through the PC point perpendicular to the AC-PC plane and the IF, the plane through the PS parallel to the AC-PC plane, the plane through the most superior point of the brain parallel to the AC-PC plane, the two planes through the most lateral points of the brain parallel to the IF, and the two planes through the most anterior and posterior points of the brain perpendicular to the AC-PC plane and the IF.

Given the transformation, A_i, of the *i*th subject's brain to the Talairach coordinate system, we then applied A_i^{-1} to each ROI defined in the Talairach proportional grid system. The resulting transformed ROI were specific to each subject *i*, but reflect a common Talairach definition. Each subject's tissue contribution to the commonly defined ROI was then computed by superimposing the subject-specific ROI on the subject's segmented image, and counting the (segmented) pixels contained in the ROI.

Statistical analysis

The seven primary imaging variables were first compared across the five groups (the entire NC sample, CN+L, CI+L, D+L, and prAD). If this overall test was significant, each lacune group and the prAD group was compared to its control group, and the lacune groups were compared to each other. The association of imaging variables with each other, and with MMSE scores, was assessed using Spearman correlations (less affected by a small number of cases than Pearson correlations). The degree to which imaging variables explained the same versus independent aspects of the differences between groups was examined using partial correlation and step-wise multiple logistic regression analyses.

An analysis of regional gray matter atrophy in the D+L and prAD groups was performed. First, the mean and SD of percent cortical gray matter in each region was computed for the single control sample that was used for both D+L and prAD groups. Each D+L and prAD subject's percent cortical gray matter in each region was converted to a Z-score, using the control sample's mean and SD for that variable. The mean Z-score for each variable for the D+L and prAD groups was then tested for difference from zero. The D+L and prAD group Z-scores for each variable were also compared by *t*-test.

Results

Demographics

Table 1 shows the age and gender comparability of each lacune group with its controls. It also illustrates that CN+L had MMSE scores comparable to its control sample ($p > 0.5$), whereas the CI+L and D+L groups had reduced MMSE scores versus their control samples ($p < 0.02$ and $p < 0.0001$). The prAD and D+L were selected to have comparable MMSE scores.

Tissue volume data

Table 1 also displays the results of the MRI tissue segmentation for all groups. There was no difference among the 5 groups (the entire NC sample, CN+L, CI+L, D+L, and prAD) in the

size of the ICV ($p > 0.3$; the ICV explained less than 3.2% of the variance in the group definition variable). All of the other primary imaging variables (WMSH percent, white matter percent, cortical gray matter percent, ventricular CSF percent, sulcal CSF percent, and hippocampal volume percent) demonstrated significant differences among the groups (accounting 24.4, 6.7, 31.3, 31.7, 14.6, and 49.6% of the variance of the group definition variable); for each of these variables, subsequent analyses were performed.

The CN+L group differed from their controls only in having a greater volume of WMSH (1.2% of the ICV versus 0.5%, $p < 0.01$). The CN+L group was comparable to their control sample on all other structural imaging measures. The CI+L group, in addition to demonstrating a greater volume of WMSH than their controls (1.4% versus 0.5%, $p < 0.01$), also evidenced cortical gray matter atrophy (percent cortical gray matter volume reduced by 4.4%, $p = 0.03$), and hippocampal atrophy (percent hippocampal volume reduced by 9.1%, $p = 0.04$). The D+L group, in addition to demonstrating a much greater extent of WMSH than their controls (2.5% versus 0.6%, $p < 0.0001$), evidenced dramatic hippocampal and cortical gray matter atrophy (-26.0%, $p < 0.0001$, and -10.9%, $p < 0.0001$) in addition to dilation of ventricular and sulcal CSF spaces ($+ 66.7\%$, $p < 0.0001$, and $+ 12.7\%$, $p < 0.025$). Percent cortical gray matter and percent hippocampal volume explained 42.7% and 48.0% of the variance between D+L and NC subjects, whereas WMSH percent, ventricular CSF, and sulcal CSF percent explained 25.1%, 31.6%, and 9.6% of the variance between the groups. When cortical gray matter and hippocampal volume measures were used together in multiple regression analyses to distinguish D+L from NC subjects, they explained 54.7% of the variance (adjusted r^2 is used throughout to index the proportion of variance explained while adjusting for the number of predictor variables). The combination of hippocampal volume with either WMSH percent or ventricular CSF percent was not significantly different from hippocampal volume and cortical gray matter percent in distinguishing D+L from NC subjects. This suggests that there was an atrophic process in the D+L group that is at least partially independent from the process leading to hippocampal atrophy, and that this process was reflected comparably in the cortical gray matter, WMSH, and ventricular CSF measures.

The CN+L versus CI+L versus D+L group comparison showed that hippocampal volume best discriminated among the lacune groups, accounting for 38.1% of the variance ($p < 0.0001$). Comparable size effects were present for ventricular CSF percent (35.8% of the variance explained, $p < 0.0001$), with smaller effects for cortical gray matter percent (17.9% of the variance, $p < 0.0005$), WMSH percent (9.3% of the variance, $p < 0.01$), and sulcal CSF percent (5.3% of the variance, $p < 0.05$). The only variables that added to hippocampal volume's ability to distinguish among the groups in multiple regression analyses were ventricular CSF percent (increasing percent variance explained to 44.2%, $p < 0.007$) and WMSH percent (increasing percent variance explained to 41.9%, $p < 0.03$); however, the proportion of variance explained by these predictor variables did not increase further when all three variables were used together. This suggests that within the lacune groups, the severity of cognitive impairment is most strongly associated with hippocampal volume reductions, but is also associated with ventricular dilation, and an increase in WMSH. Similar to the comparison between the D+L and NC groups, this suggests that there are two partially independent processes associated with the presence of cognitive impairment and dementia in subjects with lacunes. The primary process is reflected in hippocampal atrophy, and a secondary process is reflected in ventricular dilation, and to a lesser extent, in WMSH.

Table 2 shows that the number or volume of lacunes (either as a volume or as a percent of ICV) did not differentiate the CN+L, CI+L, and D+L groups ($p\text{s} > 0.40$). Similarly, none of the location-specific lacune volume measures differentiated among the lacune groups (all $p\text{s} > 0.28$). Neither the number or volume of lacunes was associated with percent cortical gray matter ($r\text{s} < 0.20$, $p\text{s} > 0.10$), percent hippocampal volume ($r\text{s} < 0.13$, all $p\text{s} > 0.30$), or with MMSE

scores (rs < 0.05, ps > 0.80). The primary structural imaging factors distinguishing the CN+L, CI+L, and D+L groups from each other were hippocampal atrophy, ventricular dilation, and an increase in WMSH (*not* lacune number, volume, or anatomic distribution).

An exploratory analysis was conducted to determine whether lacunes in specific locations (e.g., thalamus) were correlated with Talairach-defined regional cortical gray matter volumes (e.g., frontal lobe). The volume of lacunes in the putamen was associated with reduced cortical gray matter in the motor and visual cortices ($r = -0.24$, $p < 0.05$ and $r = -0.26$, $p < 0.02$). The volume of lacunes in the thalamus was associated with reduced cortical gray matter in the anterior temporal ($r = -0.22$, $p < 0.05$) and inferior temporal ($r = -0.29$, $p < 0.01$) cortices. The volume of lacunes in the caudate was associated with reduced cortical gray matter in the superior temporal cortex ($r = -0.23$, $p < 0.05$), and the volume of lacunes in the globus pallidus was associated with reduced cortical gray matter in the motor cortex ($r = -0.22$, $p < 0.05$). Given the large number of correlations computed, and the lack of control for multiple comparisons in the computation of significance levels, these correlations must be interpreted with caution.

The prAD subjects compared to their controls showed dramatic hippocampal and cortical gray matter atrophy (-34.5%, $p < 0.0001$; and -7.9%, $p < 0.0001$), and sulcal and ventricular dilation ($+ 16.6.0\%$, $p < 0.005$; and $+ 31.7\%$, $p < 0.01$). The prAD subjects did not differ from their controls on extent of WMSH ($p > 0.80$). The effect sizes as a proportion of variance explained were 62.3%, 24.0%, 13.0%, and 8.0% of the variance for hippocampal, cortical gray matter, ventricular CSF, and sulcal CSF volumes. In multiple regression analyses, no variable added to the ability of hippocampal volume to distinguish prAD from controls, suggesting one atrophic process in AD.

The prAD group compared to the D+L group tended toward relatively greater hippocampal atrophy and less cortical gray matter atrophy (ps < 0.10). The prAD subjects also had less ventricular dilation ($p = 0.03$) and a much smaller volume of WMSH ($p = 0.0005$) than D+L subjects. Figures 2, 3, and 4 present the percent WMSH, cortical gray matter, and hippocampal volume data for the prAD group versus the D+L group, and a normal control sample comparable in age and sex to both of these groups.

Association of structural imaging variables with each other, and with MMSE scores

There was a strong negative association within the combined lacune groups between the percent of WMSH and percent cortical gray matter ($r = -0.56$, $p = 0.0001$), and a weaker negative association with percent hippocampal volume ($r = -0.27$, $p = 0.03$). WMSH percent was correlated with percent cortical gray matter in every group studied ($r = -0.45$ for CN+L, -0.52 for CI+L, -0.33 for D+L, -0.42 for prAD, and -0.33 for NC; all ps < 0.05). In comparison, the correlation of WMSH percent with hippocampal percent did not reach significance in any group (all ps > 0.15).

Within the combined lacune groups, hippocampal and cortical gray matter percent were positively correlated with integrity of cognitive function as indexed by MMSE scores ($r = 0.49$, $p < 0.0001$, and $r = 0.37$, $p = 0.001$). WMSH percent was negatively correlated with the maintenance of cognitive function in the combined lacune group ($r = -0.27$, $p = 0.01$). The CN+L group had half the extent of WMSH of the D+L group ($t_{46.5} = 2.40$, $p < 0.02$).

Regional distribution of cortical gray matter atrophy

Table 3 displays the results of the analysis of regional gray matter atrophy. The D+L group had cortical gray matter atrophy compared to the control sample in all 16 regions examined. The prAD group showed atrophy compared to the control sample in all cortical gray matter regions except for the motor and visual cortices. Compared to the prAD group, the D+L group

did not evidence sparing of motor and visual cortices, and showed greater atrophy in the lateral frontal and superior temporal regions.

Autopsy data

Nine subjects have come to autopsy (table 4): eight with lacunes (four CN+L, one CI+L, three D+L) and one with prAD. The whole brain was removed at the time of death, fixed in 10% neutral buffered formalin, and sectioned coronally at 0.5 mm intervals. Tissue blocks were dissected according to CERAD,[32] consensus criteria for dementia with Lewy bodies (DLB), [33] and SIVD Program Project Protocols (unpublished). The tissue blocks were dehydrated, embedded in paraffin, sectioned, and stained with hematoxylin-eosin, cresyl-violet, Luxol fast blue, congo red, and Bielschowsky silver. In addition, immunolabeling was performed using antibodies against tau, alpha-synuclein, or ubiquitin.

Neuropathologic diagnoses were performed without knowledge of the clinical history or the MRI results. Braak and Braak stage[34] and CERAD criteria[32] were used to assess Alzheimer-type pathology. Consensus criteria were used for the diagnosis of DLB.[33] A new method was used to assess the severity and distribution of ischemic brain injury. This method provides an overall rating of the severity of cerebrovascular brain injury (CVD score) and a separate rating for the severity of ischemic brain injury that is likely, based on key location, to contribute to dementia (IVD score).[35] The type and severity of atherosclerosis, arteriosclerosis, amyloid angiopathy, and other types of microvascular disease were evaluated and scored separately.

Pathologic evidence of ischemic parenchymal brain injury was found in all eight cases with lacunes (IVD scores ranged from 5 to 19; CVD scores from 5 to 24). Neurofibrillary tangles were found in the hippocampus in four of these cases (Braak and Braak stage[34] I–IV). However, none of these cases had neurofibrillary tangles in the neocortex. Two cases showed moderate numbers of neuritic plaques; none had frequent plaques. Thus, none of the eight cases in the three lacune groups met NIA–Reagan Institute criteria supporting a high likelihood of AD.[36] The single autopsy case diagnosed clinically as prAD showed widespread Lewy bodies (LB score[33] 7), but had low likelihood that dementia was due to AD.

Discussion

Among the three SIVD groups with lacunes, we found no association between the presence or severity of cognitive impairment and characteristics of radiologically defined lacunes. That is, similar numbers, volume, and anatomic location of lacunes were found in all three groups, irrespective of their cognitive status (CN+L, CI+L, or D+L). In contrast, we observed strong associations between the severity of cognitive impairment and hippocampal atrophy, ventricular dilation, increasing WMSH, and cortical gray mater atrophy. Hippocampal atrophy has been reported consistently among patients with prAD,[10-12] but does not appear to be specific. In one study, hippocampal atrophy was also observed among nine patients with VaD. [20] The current study confirms the occurrence of hippocampal atrophy in a much larger sample of patients with D+L (three with autopsied confirmed SIVD) (see figure 4). Our data also confirm the association between dementia and ventricular enlargement, noted by other investigators studying heterogeneous samples of large- and small-artery type VaD.[3,14,15] MRI and computerized segmentation methods used in the current study enable demonstration of a stronger association between dementia in SIVD and specifically neocortical as well as hippocampal atrophy.

According to the lacunar hypothesis, dementia is related to an increasing number and volume of lacunes, particularly when strategically located in networks subserving cognition.[6,7,37] Despite our failure to marshal support for any part of this hypothesis, several caveats should be kept in mind. First, lacunes were defined, in this study, by their morphologic appearance in

MRI. Criteria were established to distinguish lacunes from perivascular spaces, and all lesions in white matter and subcortical gray matter meeting these criteria were counted and sized. However, no attempt was made to separate symptomatic from silent lacunes and only the subset of cystic lacunes was volumed in the white matter. In the absence of adequate radiologic–pathologic correlation, one should not presume that all lesions meeting radiologic criteria for lacunes are histologically comparable. A "lacune" may represent a complete infarct, incomplete infarct, area of focal gliosis, or perivascular space. Thus, the absence of correlations between cognitive impairment and numbers or volume of lacunes could be explained by the differential distribution of "false-positive lacunes" among the three lacunar groups. A preliminary review of the clinical data does not support this explanation. In our sample, 44% of our subjects with lacunes had no symptomatic history of stroke or TIA. The proportion of symptomatic versus silent lacunes, however, was evenly distributed across all three cognitive groups. Because only cystic lacunes were volumed in the white matter, our methods do not adequately address the possibility that cognitive impairment correlates with the number and volume of lacunes in the white matter.

Second, the method used in this study to localize lacunes was based upon gross anatomic boundaries, rather than functional divisions within frontal–sub-cortical loops.[37] For example, lacunes were localized to the thalamus, but not to specific nuclei such as the anterior and dorsomedial nuclei that project to the prefrontal lobe. Thus, our methods do not adequately test that component of the lacunar hypothesis related to the strategic importance of location.

Other investigators have questioned the validity of the lacunar hypothesis. No differences were found in the location or volume of lesions between demented and nondemented groups with lacunes.[3,38] Other investigators reported an association between the number, but not the volume, of lacunes and cognitive function.[17] These reports, taken together with our findings, suggest that radiologically defined lacunes, although an indicator of subcortical ischemic injury, may not be reliable markers for the overall severity of either ischemic brain injury or cognitive impairment.

The second question addressed in this study is whether dementia among patients with presumed SIVD simply indicates the presence of AD. Several pieces of evidence suggest not. The pattern of association between cognitive impairment and imaging variables differed in the lacune versus prAD groups. For the three groups with lacunes, cognitive impairment was associated with two partially independent atrophic processes. The primary process was reflected most strongly in hippocampal atrophy, whereas the secondary process was associated with greater volume of WMSH, increasing ventricular dilation, and cortical gray matter atrophy. For the prAD group, there was only evidence for one atrophic process, reflected most strongly in hippocampal atrophy. In this group, hippocampal and neocortical atrophy were strongly correlated with each other and did not contribute independently to cognitive impairment.

The regional pattern of neocortical gray matter atrophy also differed between the D+L and prAD groups. In the prAD group, primary motor and visual cortex were relatively spared. This finding is consistent with the lower densities of neurofibrillary tangles observed in these areas in histopathologically confirmed AD.[39] By contrast, in the D+L group, all regions of neocortex evidenced comparable degrees of atrophy. Several factors may limit the accuracy of Talairach transformations for defining cortical regions of interest, including increasing distortion with increasing distance from the AC-PC line and disease-specific variations in brain morphology. However, identical operations were applied to all individual brains in the study. Therefore, limitations of the method do not explain the systematic differences observed in the pattern of cortical gray matter atrophy between the D+L and prAD groups. Although some of our lacune group may yet prove to have AD (or other neuropathology) as a contributing cause of atrophy, autopsies in eight of our lacune cases confirm that hippocampal and neocortical atrophy can

and do occur in cases of relatively pure SIVD. This suggests that although cortical gray matter atrophy occurs in both AD and SIVD, the underlying cause is likely to differ.

The etiology of hippocampal and neocortical atrophy in D+L cases remains unknown. Several non-mutually exclusive possibilities may be considered: 1) concomitant AD (addressed above), 2) secondary degeneration, or 3) subclinical ischemia. Note that neurofibrillary tangles were found in the hippocampus in all three autopsied cases of D+L (Braak and Braak II–IV). In one case, hippocampal sclerosis was found as well. Thus, the pathogenesis of hippocampal atrophy in SIVD is variable and may reflect a combination of degenerative and ischemic pathologies.

Cortical atrophy in SIVD might result from secondary axonal and trans-synaptic degeneration following primary subcortical injury. This would represent the structural corollary to the traditional notion that cortical hypoperfusion in SIVD results from functional deafferentation of cerebral cortex.[40] Based on anatomic studies of frontal–subcortical circuits in nonhuman primates,[41] predominant atrophy of the prefrontal cortex might be expected. Regional analyses in our lacune groups did not reveal preferential atrophy of prefrontal cortex, as opposed to parietal, temporal, or occipital cortex (see table 3). However, despite this pattern of diffuse atrophy, secondary degeneration cannot be ruled out. Although prefrontal cortex is considered to be the primary area of connectivity, widespread areas of posterior multimodal association cortex and hippocampus are also interconnected within cortical–subcortical loops.[41]

Finally, tissue loss in neocortex might result from primary (albeit subclinical) ischemia. Occlusions of microvessels or chronic hypoperfusion might produce incomplete infarction (e.g., selective neuronal or axonal loss),[42] undetected by clinical symptomatology or by focal neuroimaging changes. Patients with severe WMSH (i.e., Binswanger type vascular dementia) may be at particular risk for subclinical ischemia. Deficient autoregulatory reserve[43] and increased oxygen extraction fraction[44-46] have been demonstrated in this subgroup of SIVD. Thus, WMSH may be a marker for the severity of deep cerebral hypoperfusion.

Several investigators have noted an association between WMSH with VaD[14] or SIVD.[16-18] In our study, WMSH volume was twofold greater in the D+L versus CN+L groups, but not significantly different in the prAD versus NC groups. In all five groups studied, WMSH volume correlated with percent cortical gray matter, but not with hippocampal volume. Among the three lacunar groups, WMSH volume correlated negatively with MMSE score. These data suggest that in SIVD, the extent of WMSH is related to the pathogenesis of dementia, as well as the magnitude of cortical gray matter atrophy. Combined with pathophysiologic data in the literature, these findings suggest that cortical gray matter atrophy may (at least partially) reflect the magnitude of an ischemic process that is indexed by the extent of WMSH, whereas hippocampal atrophy reflects yet another pathogenetic processes.

Acknowledgments

References

1. Gorelick PB, Chatterjee A, Patel D, et al. Cranial computed tomographic observations in multi-infarct dementia: a controlled study. Stroke 1992;23:804–811. [PubMed: 1595096]

2. Ross GW, Petrovitch H, White LR, et al. Characterization of risk factors for vascular dementia: The Honolulu Asia Aging Study. Neurology 1999;53:337–343. [PubMed: 10430423]

3. Loeb C, Gandolfo C, Croce R, Conti M. Dementia associated with lacunar infarction. Stroke 1992;23:1225–1229. [PubMed: 1519275]

4. Tatemichi TK, Desmond DW, Paik M, et al. Clinical determinants of dementia related to stroke. Ann Neurol 1993;33:568–575. [PubMed: 8498836]

5. Snowden DA, Greiner LH, Mortimer JA, Riley KP, Greiner PA, Markesbery WR. Brain infarction and the clinical expression of Alzheimer disease. JAMA 1997;277:813–817. [PubMed: 9052711]

6. Cummings JL. Vascular subcortical dementias: clinical aspects. Dementia 1994;5:177–180. [PubMed: 8087175]

7. Tatemichi TK, Desmond DW, Prohovnik I. Strategic infarcts in vascular dementia. A clinical and brain imaging experience. Drug Res 1995;45:371–385.

8. Román GC. Senile dementia of the Binswanger type: a vascular form of dementia in the elderly. JAMA 1987;258:1782–1788. [PubMed: 3625988]

9. Gorelick PB, Nyenhuis DL, Garron DC, Cochran E. Is vascular dementia really Alzheimer disease or mixed dementia? Neuroepidemiology 1996;15:286–290. [PubMed: 8930941]

10. Convit A, de Leon MH, Golomb J, et al. Hippocampal atrophy in early Alzheimer's disease: anatomic specificity and validation. Psychiatr Q 1993;64:371–387. [PubMed: 8234547]

11. Jack CR, Petersen RC, Xu YC, et al. Medial temporal atrophy on MRI in normal aging and very mild Alzheimer disease. Neurology 1997;49:786–794. [PubMed: 9305341]

12. Laasko MP, Soininen H, Partanen K, et al. MRI of the hippocampus in Alzheimer's disease: sensitivity, specificity, and analysis of the incorrectly classified subjects. Neurobiol Aging 1997;19:23–31.

13. Kawamura J, Meyer JS, Terayama Y, Weathers S. Cerebral hypoperfusion correlates with mild and parenchymal loss with severe multi-infarct dementia. J Neurol Sci 1991;102:32–38. [PubMed: 1856730]

14. Liu CK, Miller BL, Cummings JL, et al. A quantitative MRI study of vascular dementia. Neurology 1992;42:138–143. [PubMed: 1734295]

15. Schmidt R. Comparison of magnetic resonance imaging in Alzheimer disease, vascular dementia, and normal aging. Eur Neurol 1992;32:164–169. [PubMed: 1592074]

16. Fukuda H, Kobayashi S, Okada K, Tsunematsu T. Frontal white matter lesions and dementia in lacunar infarction. Stroke 1990;21:1143–1149. [PubMed: 2389293]

17. Corbett A, Bennett H, Kos S. Cognitive dysfunction following subcortical infarction. Arch Neurol 1994;51:999–1007. [PubMed: 7945011]

18. Sultzer DL, Mahler ME, Cummings JL, Van Gorp WG, Hinkin CH, Brown C. Cortical abnormalities associated with subcortical lesions in vascular dementia: clinical and positron emission tomographic findings. Arch Neurol 1995;52:773–780. [PubMed: 7639629]

19. Obara K, Meyer JS, Muramatsu K, Mortel KF. Lacune-associated cerebral hypoperfusion correlates with cognitive testing. J Stroke Cerebrovasc Dis 1994;4:121–129.

20. Laakso MP, Partanen K, Riekkinen P, et al. Hippocampal volumes in Alzheimer's disease, Parkinson's disease with and without dementia, and in vascular dementia: an MRI study. Neurology 1996;46:678–681. [PubMed: 8618666]

21. Folstein M, Folstein S, McHugh PR. "Mini-mental state": a practical method for grading the cognitive state of patients for the clinician. J Psychiatr Res 1975;12:189–198. [PubMed: 1202204]

22. Hughes CP, Berg L, Danziger W, Coben LA, Martin RL. A new clinical scale for the staging of dementia. Br J Psychiatry 1982;140:566–572. [PubMed: 7104545]

23. McKhann G, Drachman D, Folstein M, Katzman R, Price D, Stadlan E. Clinical diagnosis of Alzheimer's disease: report of the NINCDS-ADRDA Work Group under the auspices of Department of Health and Human Services Task Force on Alzheimer's Disease. Neurology 1984;34:939–944. [PubMed: 6610841]

24. Woods RP, Mazziotta JC, Cherry SR. MRI–PET registration with automated algorithm. J Comput Assist Tomogr 1993;17:536–546. [PubMed: 8331222]

25. SAS Institute. SAS procedures guide: version 6. SAS Institute; Cary, NC: 1990.

26. Longstreth WT, Bernick C, Manolio TA, Bryan N, Jungreis CA, Price TR, Cardiovascular Health Study Collaborative Research Group. Lacunar infarcts defined by magnetic resonance imaging of 3660 elderly people. Arch Neurol 1998;55:1217–1225. [PubMed: 9740116]

27. Pullicino PM, Miller LL, Alexandrov A, Ostrow PT. Infraputaminal lacunes. Clinical and pathological correlations. Stroke 1995;26:1598–1602. [PubMed: 7660405]

28. Watson C, Andermann F, Gloor P, et al. Anatomic basis of amygdaloid and hippocampal volume measurement by magnetic resonance imaging. Neurology 1992;42:1743–1750. [PubMed: 1513464]

29. Di Sclafani V, Bloomer C, Clark H, Norman D, Hannauer D, Fein G. Abstinent chronic cocaine and cocaine/alcohol abusers evidence normal hippocampal volumes on MRI despite cognitive impairments. Addiction Biology 1998;3:261–270.

30. Talairach, J.; Tournoux, P. 3-Dimensional proportional system: an approach to cerebral imaging. Georg Thieme Verlag; New York: 1988. Co-planar stereotaxic atlas of the human brain..

31. Bedell BJ, Narayana PA, Johnston DA. Three-dimensional MR image registration of the human brain. Magn Reson Med 1996;35:384–390. [PubMed: 8699951]

32. Mirra SS, Heyman A, McKeel D, et al. The Consortium to Establish a Registry for Alzheimer's Disease (CERAD). Part II. Standardization of the neuropathologic assessment of Alzheimer's disease. Neurology 1991;41:479–486. [PubMed: 2011243]

33. McKeith IG, Galasko D, Kosaka K, et al. Consensus guidelines for the clinical and pathologic diagnosis of dementia with Lewy bodies (DLB): report of the consortium on DLB international workshop. Neurology 1996;47:1113–1124. [PubMed: 8909416]

34. Braak H, Braak E, Bohl J. Staging of Alzheimer-related cortical destruction. Eur Neurol 1993;33:403–408. [PubMed: 8307060]

35. Chui, H.; Zarow, C.; Ellis, W., et al. Diagnosis of ischemic vascular dementia (IVD): clinical pathological correlations.. First International Conference on Vascular Dementia.. In: Korczyn, AD., editor. Monduzzi Editore; Bologna: 1999. p. 27-32.

36. The National Institute on Aging and Reagan Institute Working Group on Diagnostic Criteria for the Neuropathological Assessment of Alzheimer Disease. Consensus recommendations for the postmortem diagnosis of Alzheimer disease. Neurobiol Aging 1997;18:S1–S2. [PubMed: 9330978]

37. Cummings JL. Frontal–subcortical circuits and human behavior. Arch Neurol 1993;50:873–880. [PubMed: 8352676]

38. Loeb C. Dementia due to lacunar infarctions: a misnomer or a clinical entity? Eur Neurol 1995;35:187–192. [PubMed: 7671977]

39. Arnold SE, Hyman BT, Flory J, Damasio AR, Van Hoesen GW. The topographical and neuroanatomical distribution of neurofibrillary tangles and neuritic plaques in the cerebral cortex of patients with Alzheimer's disease. Cereb Cortex 1991;1:103–116. [PubMed: 1822725]

40. Brown GG, Garcia JH, Gdowski JW, Levine SR, Helpern JA. Altered brain energy metabolism in demented patients with multiple subcortical ischemic lesions: working hypotheses. Arch Neurol 1993;50:384–388. [PubMed: 8460960]

41. Alexander GE, DeLong MR, Strick PL. Parallel organization of functionally segregated circuits linking basal ganglia and cortex. Ann Rev Neurosci 1986;9:357–381. [PubMed: 3085570]

42. Garcia JH, Lassen N, Weiller C, Sperling B, Nakagawara J. Ischemic stroke and incomplete infarction. Stroke 1996;27:761–765. [PubMed: 8614945]

43. Kuwabara Y, Ichiya Y, Otsuka M, et al. Cerebrovascular responsiveness to hypercapnia in Alzheimer's dementia and vascular dementia of the Binswanger type. Stroke 1992;23:594–598. [PubMed: 1561693]

44. Yao H, Sadoshima S, Ibayashi S, Kuwabara Y, Ichiya Y, Fujishima M. Leukoaraiosis and dementia in hypertensive patients. Stroke 1992;23:1673–1677. [PubMed: 1440720]

45. Hatazawa J, Shimosegawa E, Satoh T, Toyoshima H, Okudera T. Subcortical hypoperfusion associated with asymptomatic white matter lesions on magnetic resonance imaging. Stroke 1997;28:1944–1947. [PubMed: 9341700]

46. De Reuck J, Decoo D, Marchau M, Santens P, Lemahieu I, Strijckmans K. Positron emission tomography in vascular dementia. J Neurol Sci 1998;154:55–61. [PubMed: 9543322]
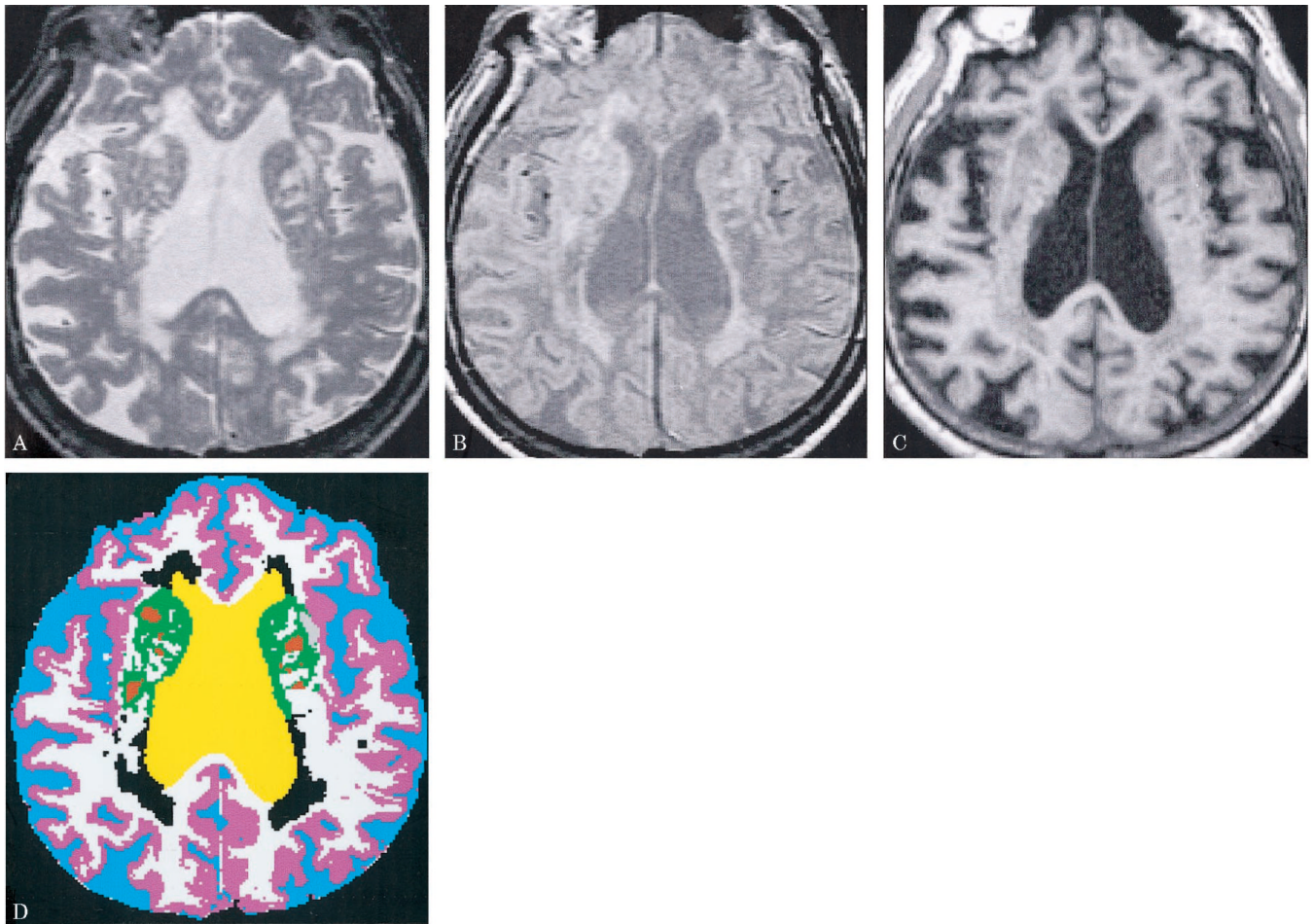
Figure 1.
MR (A, T2-weighted; B, proton density–weighted; C, T1-weighted) and segmented (D) images are presented for the midventricular axial slice of an 86-year-old man with dementia and lacunes. The segmented image (D) displays sulcal CSF in blue, ventricular CSF in yellow, cortical gray matter in pink, subcortical gray matter in green, white matter in white, white matter signal hyperintensities in black, and lacunes in red.
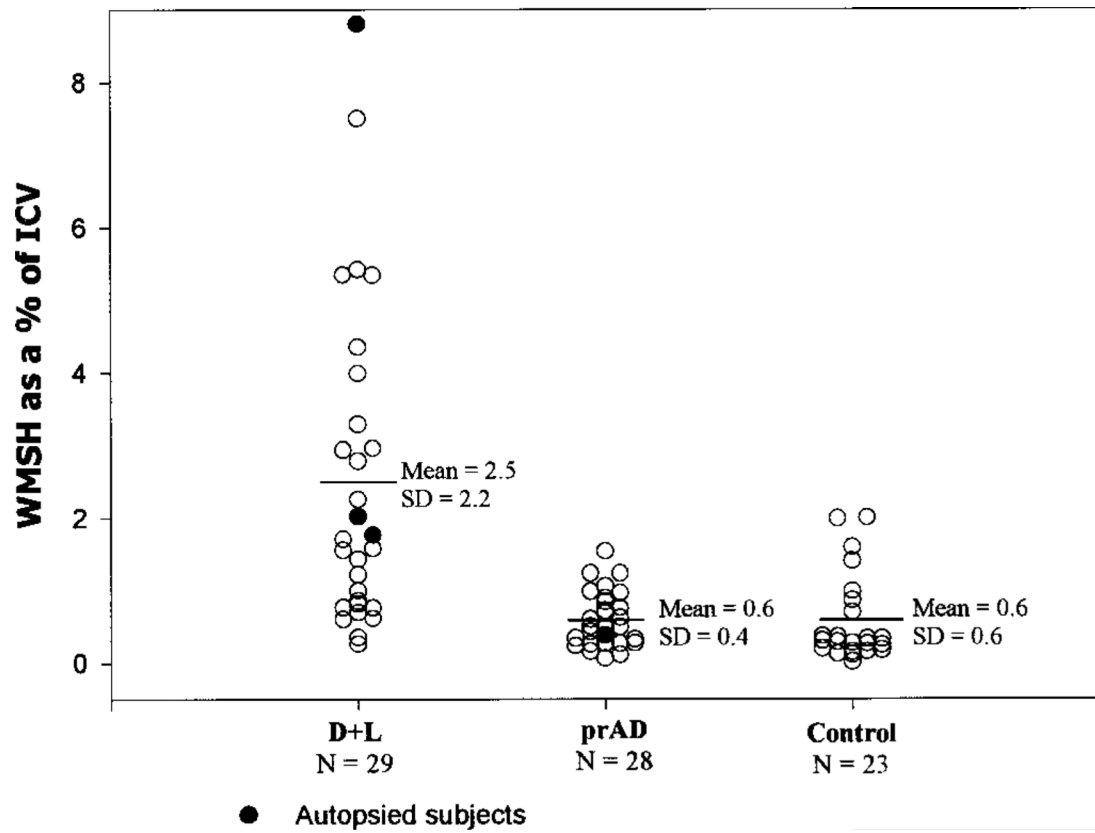
Figure 2.
Percent white matter signal hyperintensities for the dementia and lacunes (D+L), probable AD (prAD), and normal control (NC) groups.

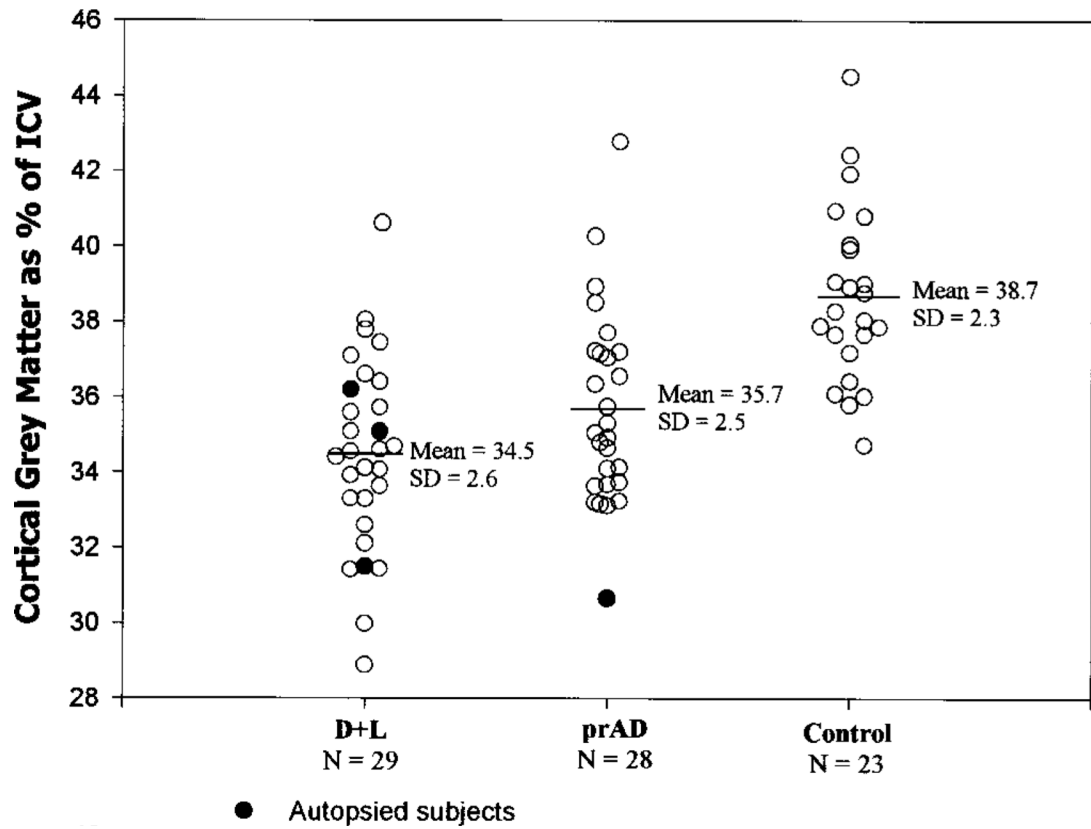**Figure 3.**
Percent cortical gray matter for the dementia and lacunes (D+L), probable AD (prAD), and normal control (NC) groups.
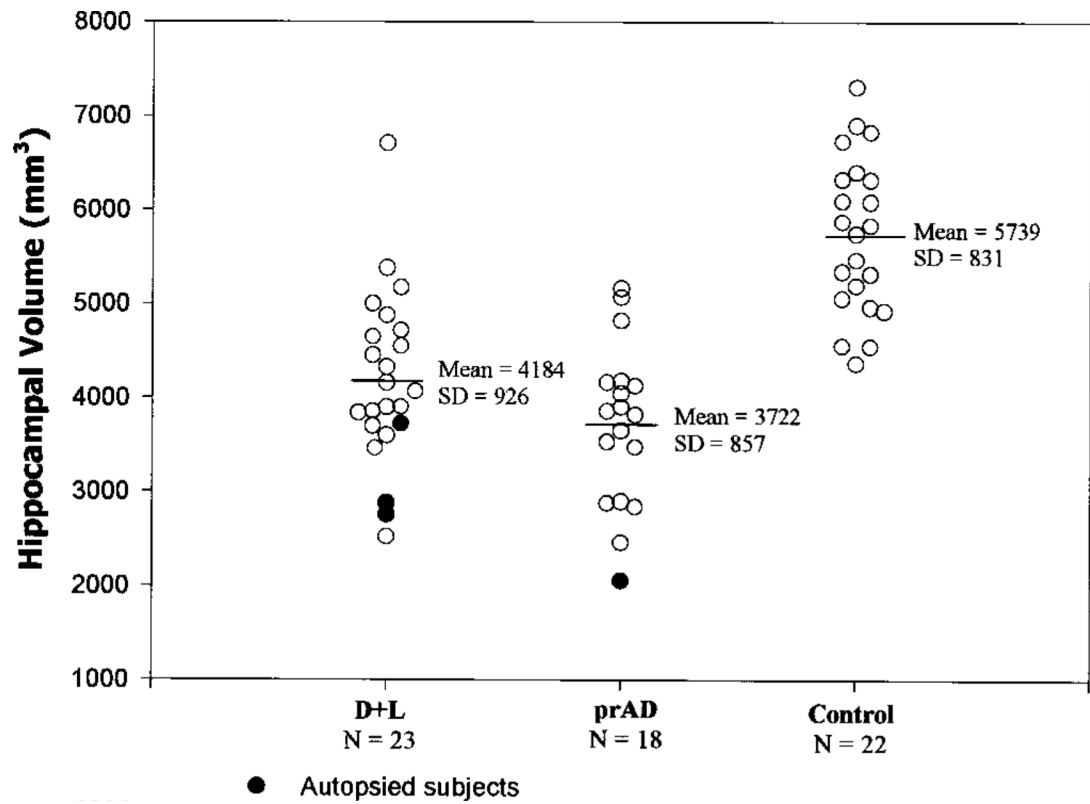
Figure 4.
Hippocampal volumes for the dementia and lacunes (D+L), probable AD (prAD), and normal control (NC) groups.

Table 1

MRI volumes for the lacune and probable AD (prAD) groups, and their respective controls

Characteristics	Cognitively normal lacune (CN +L)	Controls (NC) for CN +L	Cognitively impaired lacune (CI +L)	Controls (NC) for CI +L	Demented lacune (D+L)	prAD (demented, no lacunes)	Controls for D+L and prAD
Men/women	16/16	12/15	24/2	17/5	16/13	13/15	14/9
Age, y	75 (6)	73 (7)	72 (8)	72 (8)	77 (8)	76 (7)	76 (7)
MMSE	28.9 (1.2)	29.1 (0.9)	27.7 (2.5)*	29.1 (1.0)	21.3 (4.0)‡	21.3 (5.5)‡	29.3 (0.9)
Cortical GM %	38.1 (2.9)	39.3 (2.6)	37.1 (3.0)*	38.8 (2.2)	34.5 (2.6)‡	35.7 (2.5)‡	38.7 (2.3)
White matter %	36.2 (3.3)	36.3 (2.2)	35.0 (2.6)	35.7 (2.6)	34.5 (3.5)	33.9 (3.1)*	35.4 (2.1)
WMSH %	1.2 (1.4)†	0.5 (0.6)	1.4 (1.2)†	0.5 (0.6)	2.5 (2.2)‡[b]	0.6 (0.4)	0.6 (0.6)
Ventricular CSF %	3.9 (1.3)	3.8 (1.8)	4.7 (1.7)	4.0 (1.8)	6.8 (2.2)‡[a]	5.4 (1.9)*	4.1 (1.7)
Sulcal CSF %	20.4 (3.1)	19.3 (3.4)	21.9 (3.2)	20.2 (3.4)	23.1 (4.4)*	23.9 (4.2)†	20.5 (3.2)
Hippocampal volume, mm^3	5892 (902) (n = 12/12)	5876 (767) (n = 12/12)	5380 (894)* (n = 17/1)	5970 (834) (n = 18/1)	4184 (926)‡ (n = 13/10)	3722 (857)‡ (n = 11/7)	5739 (831) (n = 14/8)
Intracranial vault volume, cc	1322 (131)	1318 (144)	1365 (160)	1377 (127)	1289 (162)	1296 (156)	1320 (142)

Values are mean (SD). Significantly different from controls at *$p < 0.05$, †$p < 0.01$, ‡$p < 0.0001$. Significantly different from prAD at [a] $p < 0.05$, [b] $p < 0.0001$.

MMSE = Mini-Mental State Examination; GM = gray matter; WMSH = white matter signal hyperintensities.

Table 2

Lacune volumes, mean (SD) in mm^3, by lacune group[*]

Lacune location	Cognitively normal lacune (CN+L)	Cognitively impaired lacune (CI+L)	Demented lacune (D+L)
Caudate	59 (171)	55 (110)	49 (95)
Putamen	143 (219)	246 (316)	243 (310)
Globus pallidus	28 (64)	12 (24)	18 (53)
Thalamus	57 (110)	80 (124)	105 (170)
White matter	282 (851)	391 (579)	281 (544)
Total volume	570 (1212)	785 (749)	697 (817)
Volume (% of ICV)	0.041 (0.08)	0.060 (0.06)	0.057 (0.07)
Lacune number	4.4 (3.0)	6.0 (4.8)	5.5 (3.8)

[*]
No significant differences among the lacune groups were found for any of these measures (all $p > 0.28$).

Table 3

Regional cortical gray matter atrophy in the demented lacune (D+L) and probable AD (prAD) groups, compared to normal controls (NC) and to each other

Cortical region	D+L vs NC	prAD vs NC	D+L vs prAD
Frontal			
Orbital frontal and frontal pole	−16.4‡	−17.2‡	1.0
Lateral frontal	−18.0‡	−12.5‡	−6.3*
Posterior frontal	−9.4‡	−5.5†	−4.1
Superior frontal	−10.2‡	−5.0*	−5.5
Motor	−10.6‡	−1.3	−9.4†
Parietal			
Lateral parietal	−10.1‡	−10.5‡	0.5
Mesial parietal	−10.7‡	−9.6‡	−1.3
Sensory 1	−10.0‡	−6.2	−4.1
Sensory 2	−12.7‡	−8.8*	−4.3
Sensory 3	−13.5†	−10.7	−3.2
Occipital			
Anterior occipital	−15.5‡	−10.4‡	−5.6
Visual association	−12.8‡	−2.8	−10.3*
Temporal			
Anterior temporal	−16.8‡	−12.5‡	−4.9
Superior temporal	−18.9‡	−13.4‡	−6.3*
Inferior temporal	−16.5‡	−14.4‡	−2.5
Limbic lobe	−18.9‡	−12.2‡	−7.7

Values are % difference.

Significant at * $p < 0.05$, † $p < 0.01$, and ‡ $p < 0.001$.

Table 4

Summary of autopsy cases (n = 9)

No.	Clinical					Pathologic					Pathologic diagnosis
	Sex	Age, y	Sx	Group	Age at death, y	B&B	CERAD	LB	IVD/CVD scores		
1	M	75	Stroke	CN+L	77	0	None	0	16/22		IVD
2	F	74	Stroke	CN+L	78	0	0	0	5/7		IVD
3	F	82	Normal	CN+L	85	III	Rare	0	12/15		IVD/ad
4	M	73	Normal	CN+L	76	0	0	0	7/11		IVD[†]
5	M	71	Stroke	CI+L	71	I-II[*]	None	0	19/24		IVD
6	F	91	Grad	D+L	92	II-III[*]	Rare	0	9/12		IVD
7	M	79	Grad	D+L	80	III	Moderate	0	11/16		IVD/ad
8	W	76	Grad	D+L	79	IV	Moderate	0	6/9		IVD/ad
9	M	77	Grad	D	78	I[*]	Rare	7	5/5		DLB

Sx = symptomatic presentation; B&B = Braak & Braak staging; CERAD = Consortium to Establish a Registry for Alzheimer Disease; LB = Lewy Body score; IVD = ischemic vascular dementia; ad = Alzheimer-type changes confined to hippocampus; CVD = cerebrovascular disease; CN+L = cognitively normal with lacunes; Grad = gradually progressive dementia; CI+L = cognitively impaired with lacunes; D+L = dementia with lacunes.

[*] Hippocampal sclerosis.

[†] Also showed demyelinating lesions consistent with MS.